Available online at www.sciencedirect.com
ScienceDirect
Journal of Food Engineering 88 (2008) 294–305
JOURNAL OF FOOD ENGINEERING
www.elsevier.com/locate/jfoodeng

Simulation model for moving food packages in microwave heating processes using conformal FDTD method

H. Chen, J. Tang *, F. Liu

Department of Biological Systems Engineering, Washington State University, 213 LJ Smith Hall, Pullman, WA 99164-6120, USA

Received 24 October 2007; received in revised form 15 January 2008; accepted 12 February 2008
Available online 4 March 2008

Abstract

A numeric model was developed to couple electromagnetic (EM) and thermal field calculations in packaged foods moving in pressurized 915 MHz microwave (MW) cavities with circulating water at above 120 °C. This model employed a commercial EM package with a customized heat transfer sub-model to solve EM field and thermal field equations. Both methods applied finite-difference time-domain (FDTD) method. An interface was built to facilitate the communication between electromagnetic and thermal models to incorporate the coupling feature which is unique to microwave heating process. Special numerical strategies were implemented to simulate the movement of food packages. The simulation model was validated with a pilot-scale microwave system using direct temperature measurement data and indirect color patterns in whey protein gels via formation of the thermally induced chemical marker M-2. Good agreements were observed. Four cases were studied to investigate the influence of power input and package gaps on heating uniformity. These applications demonstrated the flexibility of the model to allow its usage for system and process optimization.

Keywords: Simulation; Microwave heating; Conformal FDTD method; Heat transfer; Temperature profile; Heating pattern; Food sterilization

1. Introduction

Electromagnetic (EM) energy at microwave (MW) frequencies is increasingly being used in industrial applications to increase heating rates and reduce process times as alternatives to conventional heating methods (Ohlsson, 1987, 1992). One of the major challenges in developing novel thermal processing technologies based on MW energy is non-uniform electromagnetic field distribution (Ohlsson, 1990; Ryynanen and Ohlsson, 1996). Inside a microwave cavity where microwave heating takes place, localized hot and cold spots occur due to uneven electrical field distributions. Since the process time is short, these hot and cold spots may cause severe non-uniform heating that adversely influences product quality (Ma et al., 1995; Osepchuck, 1984).

Computer simulation based on fundamental electromagnetic wave and heat transfer equations can assist the design of microwave applicators and selection of appropriate process parameters to alleviate non-uniform heating. The electric permittivity of food materials typically changes with temperature (Guan et al., 2004) at microwave frequencies, in particular at 915 MHz, a frequency allocated by FCC for high power microwave heating systems. As a result, food temperature influences microwave field distribution. Microwave heating also influences heat transfer, not only because of the generated thermal energy but also the temperature dependency of thermal properties (Zhang and Datta, 2000). That is, electromagnetic wave patterns are significantly influenced by temperature of foods, and vise versa. It is therefore critical to solve coupled electromagnetic field and heat transfer equations for a three-dimensional transient MW heating process in a practical industrial system, especially when packaged food moves.

* Corresponding author. Tel.: +1 509 335 2140; fax: +1 509 335 2722.
E-mail address: jtang@mail.wsu.edu (J. Tang).

0260-8774/$ - see front matter © 2008 Elsevier Ltd. All rights reserved.
doi:10.1016/j.jfoodeng.2008.02.020

Nomenclature

A	boundary surface area
B	magnetic flux density
C	contour path
D	electrical flux density
E	electrical field intensity (V/m)
H	magnetic field intensity (A/m)
J_i	source current density (A/m^2)
J_c	conduction current density (A/m^2)
$K(T)$	thermal conductivity at temperature T (W/m K)
Q^e	electrical charge surrounded by a surface S
S	surface for computation domain
T	temperature (°C)
T_s	circulating water temperature (°C)
μ	dielectric permeability
ε	dielectric permittivity
$c_p(T)$	specific heat at temperature T (J/kg K)
$\rho(T)$	mass density at temperature T (kg/m^3)
$\rho_v(T)$	volumetric specific heat at temperature T (J/m^3 K)
h	heat transfer coefficient (W/m^2 K)
q	thermal energy provided by circulating water on the boundary (W)
$\dot{q}$	dissipated power density provided by heating source (W/m^3)
Δx_i	cell size in x-direction (m)
Δy_j	cell size in y-direction (m)
Δz_k	cell size in z-direction (m)

The literature contains numerous reports on analytical models to describe electromagnetic fields inside domestic microwave ovens (Paoloni, 1989; Watanabe and Ohkawa, 1978; Webb et al., 1983; Shou-Zheng and Han-Kui, 1988). But only electromagnetic field distributions were considered in these studies. While Smyth (1990), Barratt and Simons (1992) considered one- and two-dimensional temperature dependent microwave heating processes, detailed treatment of three-dimensional coupled electromagnetic field and heat transfer equations has not been explored until recently. However, even these studies are limited to domestic ovens (Smyth, 1990; Zhang and Datta, 2000) or stationary cases (Bows et al., 1997; Burfoot et al., 1996; Clemens and Saltiel, 1995; Harms et al., 1996; Zhang and Datta, 2000).

Many numeric techniques can be used to solve Maxwell and heat transfer equations. Those techniques include the finite-difference time-domain (FDTD) method (Ma et al., 1995; Torres and Jecko, 1997; Pathak et al., 2003), finite element method (FEM) (Dibben and Metaxas, 1994; Webb et al., 1983) and transmission line method (TLM) (Leo et al., 1991). Of these, the FDTD method is the most popular for the coupled electromagnetic and thermal processes because it uses less computer memory and simulation time. However, for complex geometry, the FEM is often preferred; though it involves lengthy computation to inverse matrixes the size of which increases sharply with the number of elements needed to ensure accuracy (Speigel, 1984; Zhang and Datta, 2000).

The traditional FDTD method that uses staircase grids can not handle complex geometries and boundaries. The newly developed conformal FDTD algorithm overcomes this drawback by solving the integral form of Maxwell's equations. This algorithm creates finite boundary grids that conform to geometric surfaces to accurately match detailed irregularities, while retaining the simplicity of the regular grids used in the conventional FDTD algorithm for the other parts of the three-dimensional domain. A detailed description of the conformal FDTD algorithm is provided in numerous literatures (Harms et al., 1992; Holland, 1993; Madsen and Ziolkowski, 1988). Holland (1993) discussed the disadvantages of the classic staircase FDTD algorithm that significantly hindered its practical applications. Harms et al. (1992), Madsen and Ziolkowski (1988) used the conformal algorithm to accurately model the irregularities without excessive memory overhead.

In industrial microwave heating operations, food packages are transported on conveyor belts to achieve desired throughputs and improve heating uniformity along the moving direction. However, no numeric model has been reported in the literature to deal with load movement for industrial microwave applications. The current study extends the coupled model described by Chen et al. (2007) that used conformal FDTD algorithms for electromagnetic field simulation and conventional FDTD method for thermal field to simulate microwave heating of moving food packages in continuous industrial microwave sterilization and pasteurization processes.

2. Problem statement

The industrial system we attempted to model in this study was a single-mode 915 MHz MW sterilization system developed at Washington State University (Tang et al., 2006). A simplified version of this system is described in details by Chen et al. (2007). In brief, the system consisted of four sections: two MW heating sections in the center, and a loading section and a holding section on each end (Fig. 1). MW energy was provided by two 5 kW generators operating at 915 MHz, each connected by standard waveguides WR975 (Fig. 2) that supported only TE_{10} mode to a T-split (not shown in Fig. 1). Fig. 3a and b shows a close-up front and top view, respectively, of the MW heating section, which consisted of a rectangular cavity with one horn shaped applicator on the top and an identical

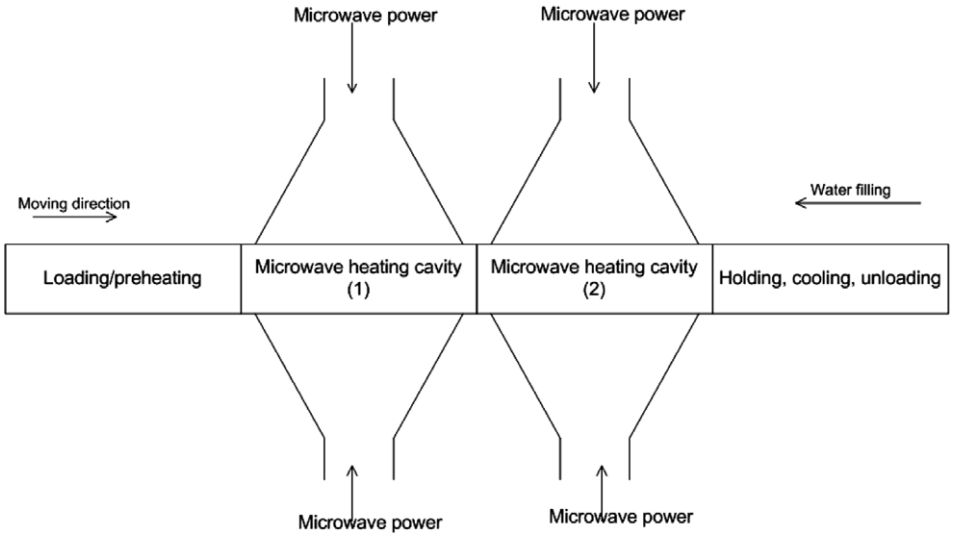

Fig. 1. Continuous microwave heating system (front view).

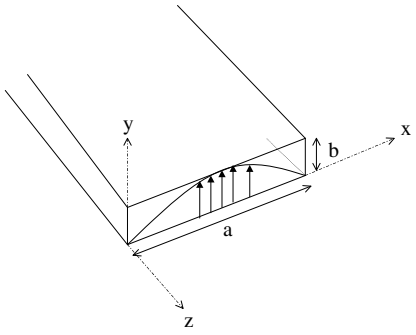

Fig. 2. Geometrical configuration of single-mode waveguide with dominant mode TE_{10}.

applicator on the bottom. The loading and holding sections were also rectangular cavities. Microwaves of equal intensity after the split were directed to the entry ports of the top and bottom horn applicators of each cavity. The length of the waveguides could be adjusted to regulate phase difference between the two waves entering the top and bottom applicators, which affected the EM field distribution inside the MW cavity and the food being heated. It was therefore possible to improve the heating uniformity by properly adjusting the phase shift between the two waves to achieve the desired field distribution in each cavity (Balanis, 1989; Jurgens et al., 1992). For simplicity, the model described here was limited to zero phase shift between the entry ports

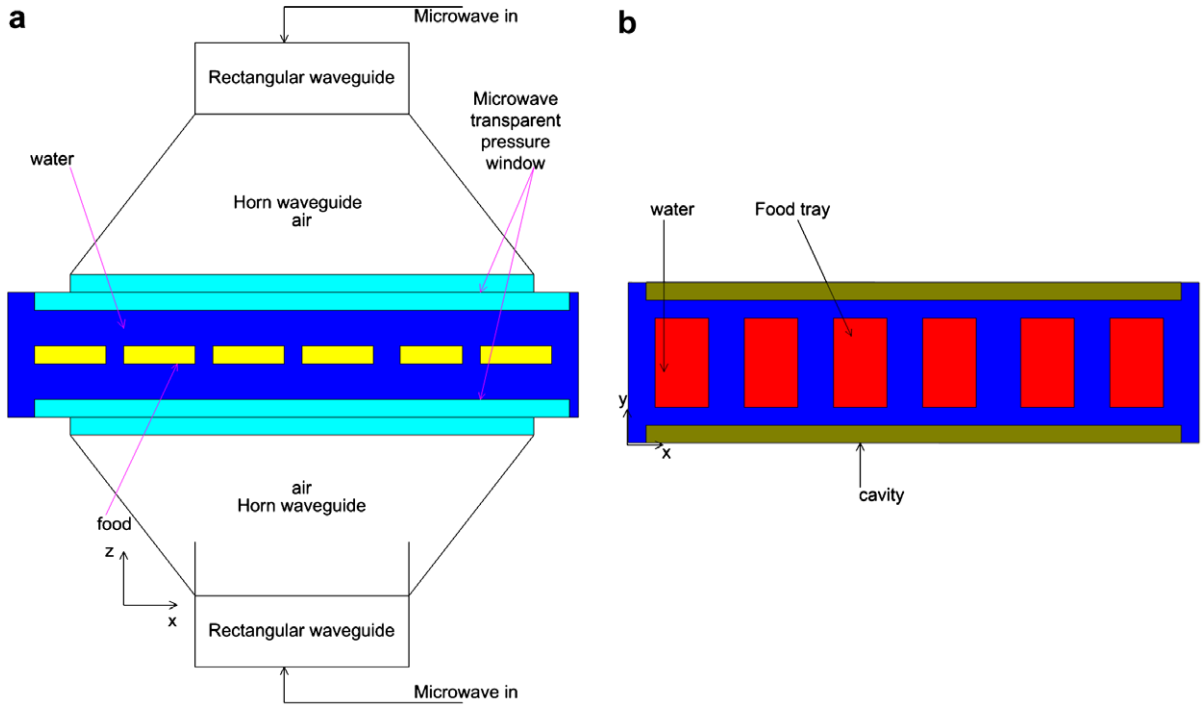

Fig. 3. Schematic view of one microwave section: front view (left) and top view (right).

of the top and bottom horn applicators for both cavities, though the model could be extended to general case with arbitrary phase differences. To achieve zero phase shifts, two pieces of waveguides with quarter wavelength each were added to one path after the T-split so that the interacting waves had the same phase in the central plane of the cavity.

The pilot system included both circulating hot water to provide heating from outside food packages and MW sources for volumetric heating, which significantly improved heating uniformity and reduced processing time. The temperature of the circulation water in the cavity was set at 125 °C, and the food temperature at cold spots reached over 121 °C to ensure that low-acid foods (pH > 4.5) were properly processed as shelf-stable products. The depth of the water was the same as the depth of microwave cavity. An overpressure of 276 kPa was provided through a buffer tank to prevent water from boiling at 125 °C and prevent packages from bursting due to internal vapor pressure. At the base of the top and bottom horn shaped waveguides, two MW-transparent windows were secured to keep pressurized hot water from entering the waveguides. During continuous thermal processing, packaged food was moved from the loading section through the two MW heating sections to the holding section.

3. Fundamentals for numerical modelling

3.1. Governing equations for EM field

The EM fields were calculated using the conformal FDTD algorithm based on the integral form of Maxwell's equations (Balanis, 1989; Jurgens et al., 1992):

$$\oint_{\mathrm{c}} \vec{E}\cdot \mathrm{d}\vec{l} = -\frac{\partial}{\partial t}\iint_s \vec{B}\cdot \mathrm{d}\vec{s} \tag{1}$$

$$\oint_{\mathrm{c}} \vec{H}\cdot \mathrm{d}\vec{l} = \frac{\partial}{\partial t}\iint_s \vec{D}\cdot \mathrm{d}\vec{s} + \iint_s (\vec{j}_i + \vec{j}_{\mathrm{c}})\cdot \mathrm{d}\vec{s} \tag{2}$$

$$\oiint_s \vec{D}\cdot \mathrm{d}\vec{s} = Q^{\mathrm{e}} \tag{3}$$

$$\oiint_s \vec{B}\cdot \mathrm{d}\vec{s} = 0 \tag{4}$$

where $\vec{E}$ is the electric field, $\vec{H}$ is the magnetic field, $\vec{D} = \varepsilon\vec{E}$ is the electric flux density, $\vec{B} = \mu\vec{H}$ is the magnetic flux density. Q^{e} is the electric charge surrounded by surface S. μ and ε are the permeability and permittivity, respectively. The permeability μ is assumed equal to free space value μ_0. The dielectric permittivity $\varepsilon = \varepsilon_0\varepsilon_r = \varepsilon_0(\varepsilon_r' - j\varepsilon_r'')$. C is a contour path surrounding the surface S. J_i and J_{c} are source current density and conduction current density, respectively.

The Maxwell's equations in the integral form were solved by a commercial electromagnetic solver QuickWave-3D (QW3D, Warsaw, Poland) using the conformal FDTD algorithm (Gwarek et al., 1999; Taflove, 1998). The advantage of the conformal FDTD algorithm over conventional FDTD has been discussed in detail by Taflove (1998).

3.2. Governing equations for heat transfer

Since the MW heating process considered in this study included heating from MW energy and circulating hot water, the EM fields were coupled with heat transfer equations to take into consideration the temperature dependent dielectric properties. For the thermal field calculations, heat conduction was assumed to take place inside the food package while convective boundary conditions were applied to the food surface to take into account the effect of the circulating water in the system. The heat transfer equation and its boundary condition are as followings (Incropera and DeWitt, 2001):

$$\frac{\partial T}{\partial t} = \frac{1}{\rho_{\mathrm{v}}(T)}\nabla(K(T)\cdot\nabla T) + \frac{\dot{q}}{\rho_{\mathrm{v}}(T)} \tag{5}$$

$$q = hA(T_{\mathrm{s}} - T) \tag{6}$$

where $K(T)$ is thermal conductivity, $\rho_{\mathrm{v}}(T) = \rho(T)c_p(T)$ is volumetric specific heat, $\rho(T)$ is mass density, $c_p(T)$ is specific heat, q is thermal energy provided by circulating water on the boundary, h is heat transfer coefficient of 220 W/m^2 K, A is the boundary surface area and T_{s} is circulating water temperature. $\dot{q}$ is derived from the root mean square value of electrical field:

$$\dot{q}(r,T) = 2\pi\varepsilon_0 f\varepsilon_r''(T)\left[\frac{\int_V(\vec{E}*\vec{E})\,\mathrm{d}V}{2V}\right] \tag{7}$$

To be consistent with the EM model and in order to simplify the mathematical computation, the heat transfer equation was solved numerically using the FDTD method. We only considered semi-solid or solid foods in which heat conduction was the dominant heat transfer mode. The heat conduction equation (5) was differentiated as

$$\begin{aligned} T^{n+1}(i,j,k) &= \left(1-\alpha_t\left(\frac{2}{\Delta x_{i-1}\Delta x_i}+\frac{2}{\Delta y_{j-1}\Delta y_j}+\frac{2}{\Delta z_{k-1}\Delta z_k}\right)\right)T^n(i,j,k) \\ &+\alpha_t\left(\frac{T^n(i+1,j,k)}{h_{x_i}\Delta x_i}+\frac{T^n(i-1,j,k)}{h_{x_i}\Delta x_{i-1}}+\frac{T^n(i,j+1,k)}{h_{y_j}\Delta y_j}\right. \\ &\left.+\frac{T^n(i,j-1,k)}{h_{y_j}\Delta y_{j-1}}+\frac{T^n(i,j,k+1)}{h_{z_k}\Delta z_k}+\frac{T^n(i,j,k-1)}{h_{z_k}\Delta z_{k-1}}\right)+\frac{\dot{q}\Delta t}{\rho_{\mathrm{v}}} \end{aligned} \tag{8}$$

where Δx_i, Δy_i, Δz_k cell sizes are in x-, y-, z-direction, respectively. $\rho_{\mathrm{v}} = \rho c_p$ $\alpha_t = \frac{K\Delta t}{\rho_{\mathrm{v}}}$. Here, ρ_{v} and α_t are functions of $T^n(i,j,k)$. We drop subscription for better presentation. h_x, h_y, h_z are defined as the mean value of adjacent cell sizes in the x-direction, y-direction and z-direction, respectively:

$$h_{x_i} = (\Delta x_i + \Delta x_{i-1})/2, \quad h_{y_j} = (\Delta y_j + \Delta y_{j-1})/2,$$
$$h_{z_k} = (\Delta z_k + \Delta z_{k-1})/2 \tag{9}$$

The temperature responses at food surface nodes served as the interface between conduction heat (interior nodes) and convection heat (circulation water). Therefore, the

finite difference form for the heat transfer equation was slightly modified on the surface nodes by replacing the conduction term in Eq. (8) with corresponding convective term. For example, for the nodes on the top surface of food package (parallel with x–y plane), the difference form in Eq. (8) for the boundary condition was modified by using $q = h * \Delta x_i * \Delta y_j * [T_s - T^n(i,j,k)]$ to replace the conduction term $[T^n(i,j,k+1) - T^n(i,j,k)] * K(T) * \Delta z_k$.

3.3. Numerical mode for simulating moving package

In MW heating process with moving packages, food packages enter the heating chamber in sequence. However, conducting computer simulation for all moving food packages in the microwave cavities would have involved dynamically allocating and re-allocating a large amount of memory several times during each simulation process and transferring computation information back and forth between internal memory and external disk storage. In addition, since the focus of this study was on the heat distribution inside a representative moving food package, the simulation model solved the coupled equations at the grids inside the selected food package, while only EM field patterns were calculated for domains outside of this food package boundary.

The EM field patterns were assumed not to influence the temperature distribution of circulating water because of the large flow rate (~130 L/min). The simulation model traced the temperature profile of the single food package at equally spaced positions as it traveled through the heating cavities. The temperature distribution calculated for the package at one position served as the initial condition for its next position.

The simulation considered two different stages: (1) food package heated by circulating water in the loading section; and (2) simultaneous MW and surface water heating when food packages moved through the two MW heating sections. At the first stage, only heat transfer equations were used to calculate the temperature distribution, as a result of surface hot water heating, this temperature distribution was then used as the initial condition for the second stage to calculate the temperature response from the combined hot water and MW heating.

The MW power density in the packages at a particular position was calculated from Maxwell's equations using temperature-dependent dielectric properties. Since the EM process is much faster than the thermal process, its steady state was established before the thermal reaction took place and the field intensity within the food package was assumed constant until the package was moved to its subsequent position. Temperature response was then calculated by the heat transfer sub-model with constant power density at each node for each time increment between the two positions. At the next position, the temperature-dependent dielectric properties and thermal properties were recalculated based on the temperature of each element in the food package in consideration. When the food package traveled from one MW chamber to the other, the geometry and mesh layout generated in QW3D for the EM computation were modified automatically to adapt to the different system configuration. During simulation, the generated mesh information used for EM calculation was kept in an external file readily accessible by the thermal model, so that the mesh grids used for numeric solutions of the Maxwell's equations and thermal equations were consistent, thus dramatically reducing the complexity of mathematical manipulations. Temperature dependent dielectric and thermal properties of the food used in the experiment were updated in the simulation package by using interpolation techniques from the properties measured at distinct temperatures. This coupled calculation loop continued until the required heating time was reached. Fig. 4a presents the simulation scheme for the coupled model. The node transformation procedure in Fig. 4b was used to exchange the data between the computational nodes for thermal energy generation due to MW heating and computational nodes for EM field updates due to thermal effects.

3.4. Node transformation

The simulation model consisted of two node transformation blocks necessary to facilitate the communication between the QW3D and customized heat transfer model (Kopyt and Celuch-Marcysiak, 2003). The temperature nodes were defined on grid lines while the nodes for EM energy generation from microwaves (used in QW3D to calculate the power distribution) were located in the center of each FDTD cell. This layout avoided the numerical instability of the heat transfer model, which might occur otherwise. The node transformation included two steps in sequence. The first step was to re-distribute the calculated EM energy from the center node to the temperature nodes at the corners of the FDTD cell. For each temperature node, the contributions of EM energy from its adjacent cells were added to compute temperature increase using the heat transfer model. The second step was to calculate the temperature associated with the EM nodes used in QW3D for the next EM field computation. For each single cell, only temperature nodes at the corners were assumed to contribute to the dielectric change. The following two equations show the mathematic manipulations for the first and second steps, respectively:

$$\begin{aligned} q_r(i,j,k) = {} & [q(i,j,k)\Delta x_i\Delta y_j\Delta z_k + q(i-1,j,k)\Delta x_{i-1}\Delta y_j\Delta z_k \\ & + q(i,j,-1,k)\Delta x_i\Delta y_{j-1}\Delta z_k + q(i-1,j-1,k)\Delta x_{i-1}\Delta y_{j-1}\Delta z_{k-1} \\ & + q(i,j,k-1)\Delta x_i\Delta y_j\Delta z_{k-1} + q(i-1,j-1,k-1)\Delta x_{i-1}\Delta y_{j-1}\Delta z_{k-1} \\ & + q(i,j-1,k-1)\Delta x_i\Delta y_{j-1}\Delta z_{k-1} + q(i-1,j-1,k-1) \\ & \times \Delta x_{i-1}\Delta y_{j-1}\Delta z_{k-1}]/(8h_{x_i}h_{y_j}h_{z_k}) \end{aligned} \tag{10}$$

$$\begin{aligned} T_q(i,j,k) = {} & [T(i,j,k) + T(i-1,j,k) + T(i,j-1,k) + T(i-1,j-1,k) \\ & + T(i,j,k-1) + T(i-1,j,k-1) + T(i,j-1,k-1) \\ & + T(i-1,j-1,k-1)]/8 \end{aligned} \tag{11}$$

where $q_T(i,j,k)$ is the dissipated power associated with the temperature node $T(i,j,k)$. Eq. (10) was used for the first

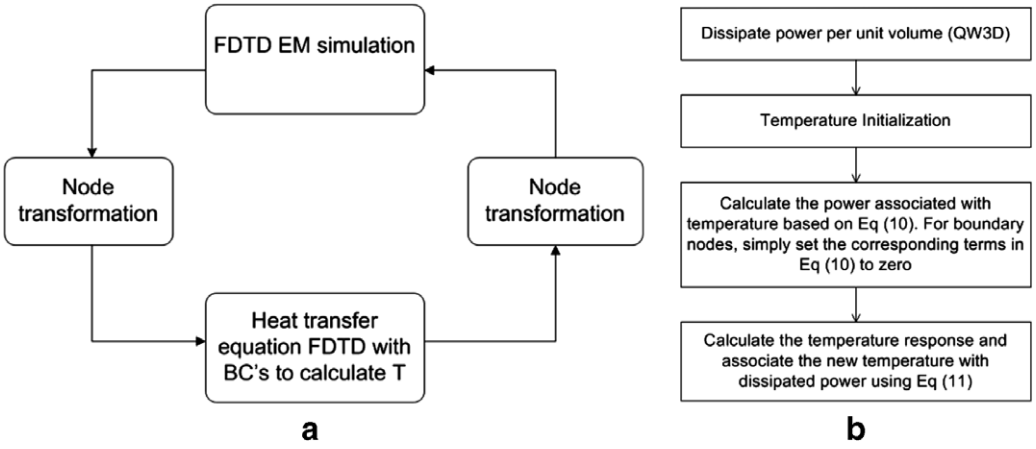

Fig. 4. Coupled model for microwave heating: (a) numeric schema and (b) communication flowchart.

step and could be applied to nodes on the boundary or inside food package. For the terms where the index number (i,j,k) exceeded the specified computation domain, they were simply replaced by zero. Eq. (11) was used for the second step, where T_q (i,j,k) is the temperature at cell (i,j,k) associated with dissipated power node. The complete algorithm is presented in the following diagram Fig. 4b.

4. Experimental methods

4.1. Temperature history and heating pattern determination

The Pilot-scale MW system shown in Fig. 1 was used to validate the model. During the experiment, one optic sensor that traveled with the food packages was placed at the cold spot predetermined by a chemical marker method (Pandit et al., 2007a,b). This method measured color changes in response to formation of a chemical compound (M-2) due to a Millard reaction between the amino acids of proteins and a reducing sugar, ribose. The color response depended on the heat intensity at temperatures beyond 100 °C and, therefore, served as an indicator of temperature distribution after MW heating. Detailed information about the kinetics of M-2 formation with temperature can be found elsewhere (Lau et al., 2003; Pandit et al., 2006). After MW processing, the heating patterns inside the whey protein gels were obtained with computer vision software IMAQ (National instrument, TX, USA) using a computer vision method described in Pandit et al. (2007b).

4.2. Processing of model food

To minimize the experimental error, it was desirable to use a model food that could be made with consistent dielectric and thermal properties. Its shape also needed to be easily maintained during the heating process so that the fiber optic sensor could be secured to a fixed position in the food. For these reasons, preformed whey protein gels (78% water, 20% protein, 1.7% salt, 0.3% D-ribose) sealed in a 7 oz polymeric tray (140 mm × 95 mm × 16 mm) were selected as a model food in our experiment. The gels were made by mixing 78% water, 20% protein, 1.7% salt, and 0.3% D-ribose; the mixtures were heated in a container in a water bath at 80 °C for about 30 min until solidification; the gels were then stored in refrigerator at 4 °C over night. The dielectric properties of the whey protein gels at the different temperatures shown in Table 1 were measured by an HP8491B network analyzer (Hewlett–Packard Company, CA, USA) using an open coaxial cable. The double needle method (Campbell et al., 1991) was used to measure the thermal properties (Table 2) with a KD2 device (Decagon, WA, USA). Since the hot water was pumped into the cavity at 40 L/min, its temperature was assumed uniform at the temperature of 121 °C during the whole process. The dielectric properties of the hot water were measured also using an HP8491B network analyzer. For the sterilization purpose, food temperature needs to reach 121 °C (Guan et al., 2004).

Table 1
Dielectric properties of whey protein gel

Temperature (°C)	Dielectric constant $\varepsilon'_r = \varepsilon'/\varepsilon_0$	Dielectric loss $\varepsilon''_r = \varepsilon''/\varepsilon_0$
20	58.50	24.25
40	57.55	30.25
60	56.36	36.79
80	54.36	45.21
100	52.81	53.89
121	51.14	63.38

Table 2
Thermal properties of whey protein gel

Temperature (°C)	Volumetric specific heat, ρc_p (MJ/m^3 K)	Thermal conductivity, K (W/mK)
0	3.839	0.513
20	3.973	0.537
35	3.901	0.550
50	3.814	0.561
65	3.883	0.578
80	3.766	0.588

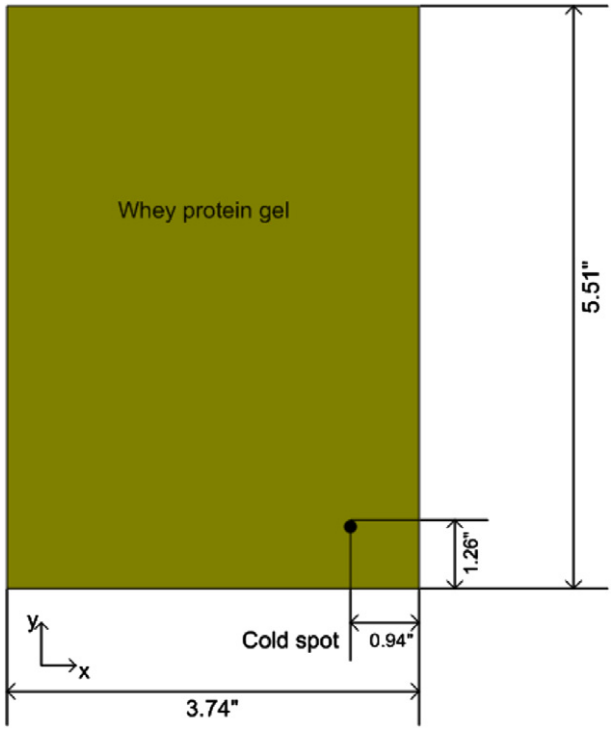

Fig. 5. Top view of middle layer of whey protein gel inside a 7 oz tray with fiber optic sensor at cold spot.

Prior to the experiment, the packaged whey gel slab (95 mm × 140 mm × 16 mm) was stored in a refrigerator at 9 °C overnight. Fig. 5 shows the location of the cold spot where a pre-calibrated fiber optic sensor [FOT-L, FISO, Québec, CANADA] was inserted carefully with proper seal at the tray wall entry port to prevent water leakage.

For MW processing, the tray with the probe was placed in the middle of five other trays without probes on a conveyor belt in the loading section. The pressure door was closed, and hot water at 125 °C at 276 kPa gauge pressure was introduced in the opposite direction to that of the tray movement (from the holding section to the loading section). When the temperature at the cold spot in the trays reached 60 °C, they started moving in the preheating section and through two microwave heating sections at a predetermined belt speed (0.3 in./s) so that the temperature at the cold spot could reach a minimum of 121 °C. When the last of the six trays moved outside of the two MW heating section, microwave power was turned off, and 12 °C tap water was pumped into the cavities to replace the hot water and cool the food packages.

To focus more on the effect of microwave energy on the heating performance, the middle layer of the gel sample was selected to reveal the heating pattern using chemical marker with computer imaging system because the middle layer was heated the least by circulation hot water as compared to other parts in the tray. The color image at the middle layer of the whey protein gel was taken with its intensity correlated with heating intensity. The heating pattern was then obtained by using IMAQ.

5. Model verification and discussion

5.1. Computer model implementation

In simulating a MW heating process for moving packages, only one food tray was chosen to model coupled EM and heat transfer to reduce computer memory usage. In the simulated system, six trays shown in Fig. 3 were considered to represent six different snapshots at different time steps for one tray. For each different step, the dissipated power distribution inside the food package was put into the heat transfer model to calculate the heat distribution. The time step was determined from the tray moving speed and spatial distance between adjacent snapshots, i.e., the distance between the centers of two neighboring trays.

A sine wave at frequency of 915 MHz was used as the excitation and its amplitude was the square root of input power (2.7 kW in this study). The rectangular waveguide shown in Fig. 2 was configured to support the propagating wave with TE_{10} mode. The MW sections had open ends on right and left sides, which then required the numeric model to terminate with proper absorbing boundary conditions (ABC). However, Chen et al. (2007) concluded that both perfect electrical conductor (PEC) and ABC leaded to similar simulation results with the maximum error less than 5%. It was argued that the PEC boundary condition was more suitable for simulating this system because it involved less mathematical manipulation. Therefore, instead of ABC, two PEC metals were imposed on the left and right ends of MW cavity to reduce the complexity of system modification for moving food package.

5.2. Validation results

A detailed convergence study for simulating a MW sterilization system with stationary packages was reported as well as the validation of a heat transfer model by Chen et al. (2007). To verify that the model correctly simulates a MW heating process involving moving packages, the simulated heating pattern and temperature profile were compared with experimental results. The temperature profiles measured with a fiber optical sensor in two identical experiments are presented in Fig. 6, along with the simulated result. Both experiment and simulated results show the temperature change with time along the moving direction. In the preheating section without microwaves, food package with initial temperature of 9 °C was heated by hot water at 125 °C. Because of the large gradient of temperature between food package and hot water, product temperature increases rapidly. The temperature difference between product and surrounding water, however, decreases as the temperature of food package goes up, resulting in lower heating rate especially at the cold spot. The heating rate at the cold spot becomes infinite small when the temperature approaches to 121 °C. The microwave heating was used in our system to sustain continued temperature increase beyond the initial heating after the

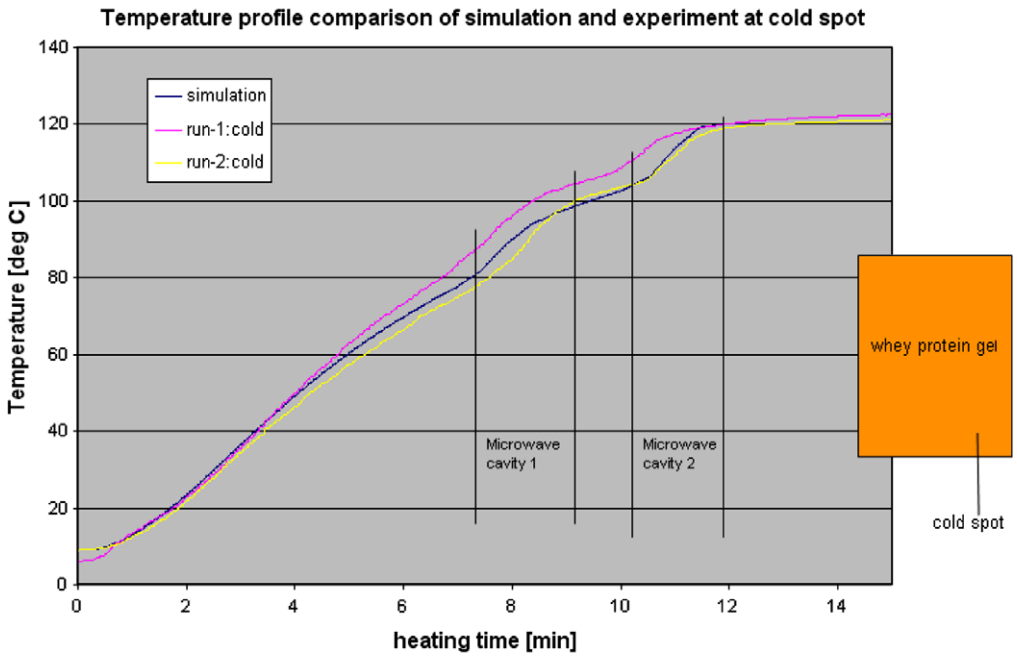

Fig. 6. Comparison of simulation results for temperature evolution at cold spot with experiment results from two identical experimental runs.

driving potential due to conventional heat transfer becomes small. The heating rate decreased when food moves out from the microwave heating cavity (1) (Fig. 1) and increases again after food enters into the microwave heating cavity (2). Fig. 7a and b compares the heating patterns from the experiment and simulation, respectively. Fig. 7a shows the temperature distribution calculated from the simulation, while Fig. 7b shows the color of the measured heating pattern reflected by chemical marker M-2 using the computer vision method, which indicated the heat intensity inside food packages after microwave heating process. The two are similar, indicating the locations of hot and cold spot were accurately predicted by the numeric model.

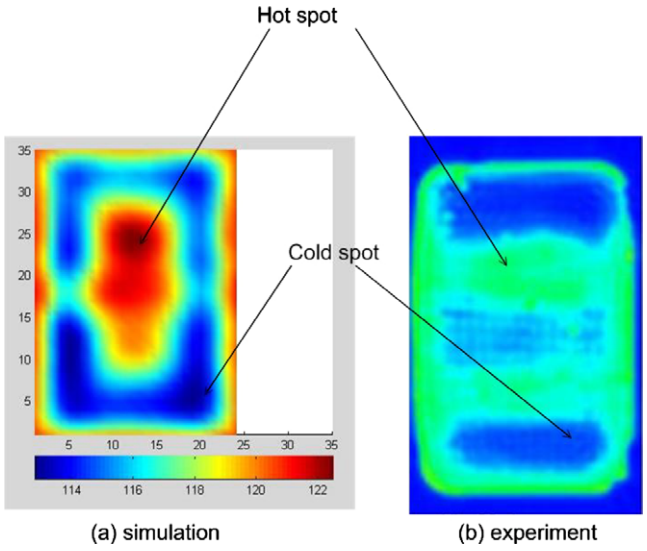

Fig. 7. Final snapshot of temperature distribution from simulation (a) and accumulated heating pattern reflected by color image from chemical marker (b) at the middle layer of whey protein gel (top view) after 3.2 min MW heating time.

5.3. Discussion

The simulated temperature profile in Fig. 6 clearly shows that the food package was traveling from the preheating zone at product of 9 °C to the unloading zone at product of 121 °C (Fig. 1) during the heating process. It generally agrees with the measurements from two duplicated experiments. The measurements were not perfectly matched because it is impossible to conduct two experiments that are exactly same. In addition, the fiber optical sensor could not be placed at the exact location as specified in the simulation. For example, if the fiber optical sensor happened to be placed closer to the hot area, the measured temperature profile would be like the higher curve compared to that of the simulated one in Fig. 6. Similarly, if location of fiber optical sensor was closer to the physical cold spot than that specified in the simulation, the measured temperature profile should correspond to the lower curve presented in Fig. 6.

Usually, for MW sterilization and pasteurization applications, the final temperature of foods after a heating process at a cold spot is more important than the intermediate temperatures during the process. The final temperatures from three curves in Fig. 6 have discrepancies less than 1 °C. Fig. 7 shows that the temperature distribution from simulation and the heating patterns obtained from the experiment are similar; especially the locations of hot and cold spots were correctly predicted by the numerical model. The main reason for the disagreement between simulated

Table 3
Case study of heating uniformity

	P_1 (kW)	P_2 (kW)	L (in.)
Case 1	2.7	2.7	1.25
Case 2	5.0	2.0	1.25
Case 3	2.7	2.7	2.5
Case 4	5.0	2.0	2.5

and measured patterns was that the obtained simulation image was a final snapshot of temperature distribution for the moving package while the measured heating pattern was an accumulated result reflected by a color image from a chemical marker. Another reason was that the water floatation made it impossible in reality to control the middle layer of the gel during heating process, especially when

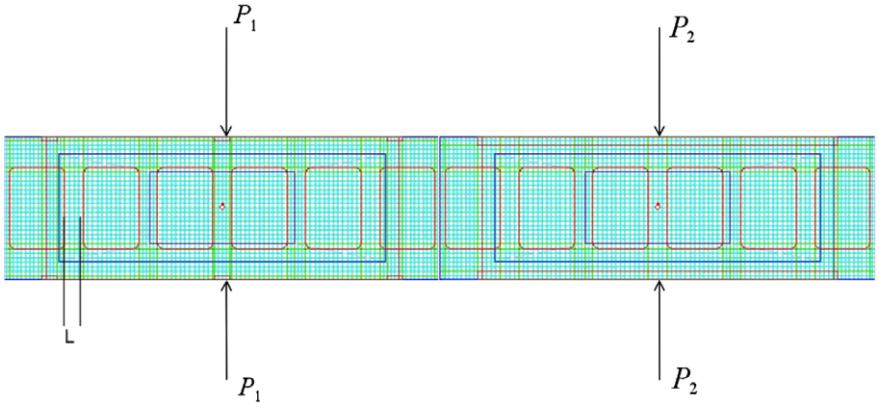

Fig. 8. Arrangement of simulation for moving packages at several cases.

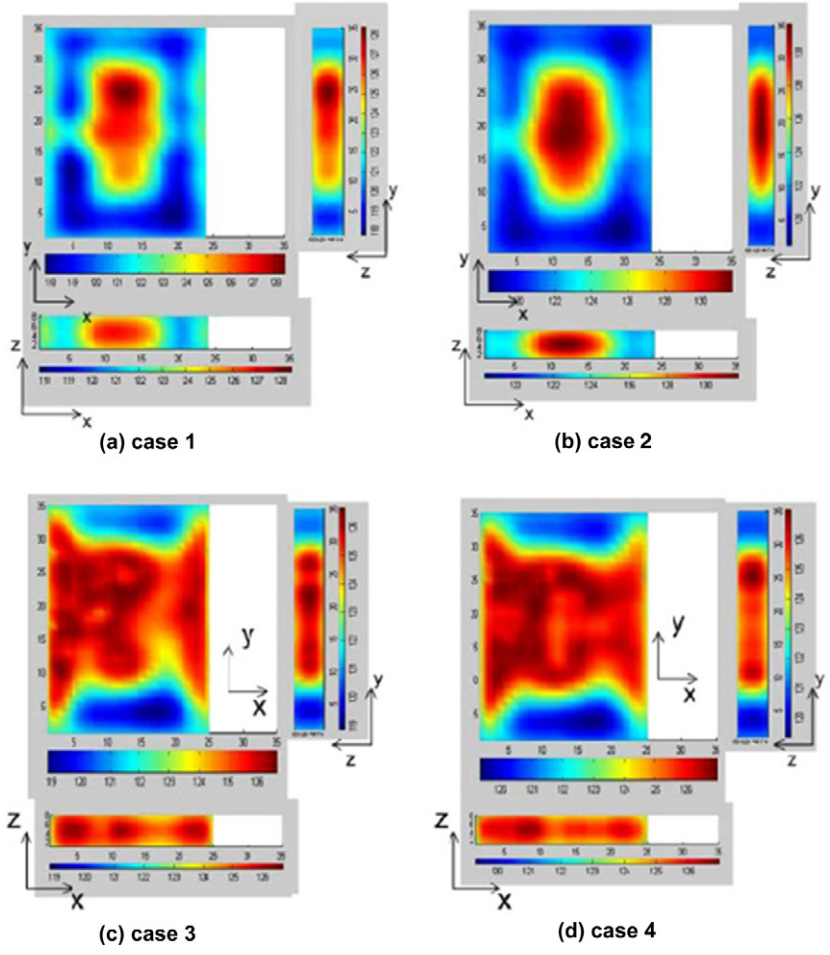

Fig. 9. Temperature distribution (°C) at the middle layer from top, front and side view for different cases.

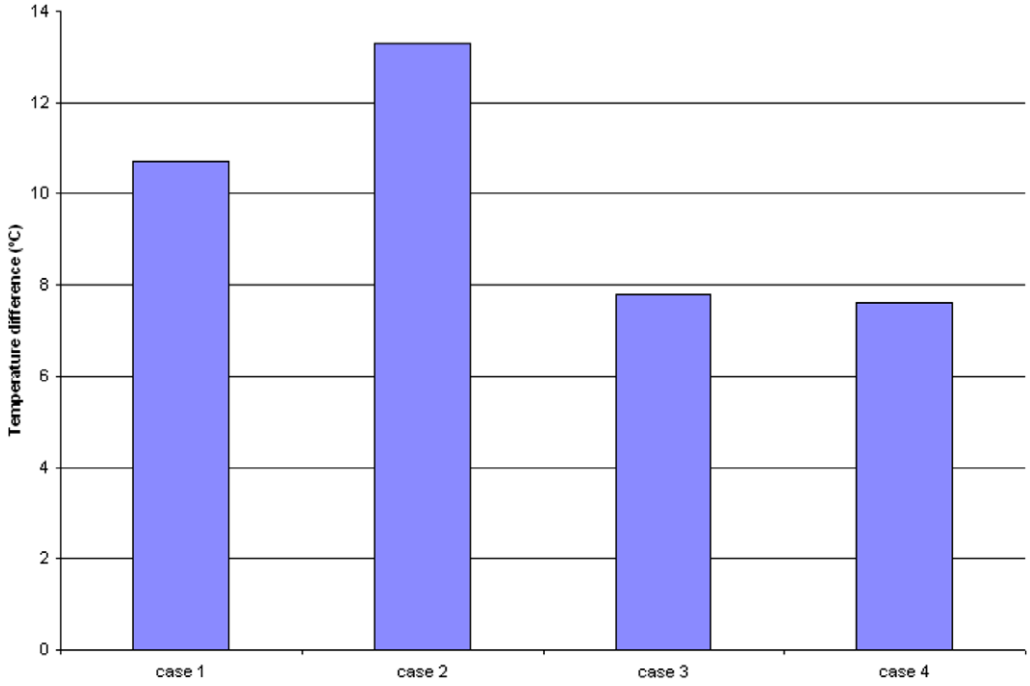

Fig. 10. Heating uniformity at the middle layer of whey protein gel.

package was moving. Instead, during simulation, the gel was assumed to stay in the middle of the cavity in the z-direction all the time. While the whole temperature distributions were compared in Fig. 7, the simulated and measured temperature profile at the cold spot was presented in Fig. 6, which is critical to our application. In addition, because of the complexity of the problem, the developed numeric model was more employed to be an indicator of the heating pattern after process that roughly located the critical points to minimize the experiment efforts.

6. Model applications

One important criterion for heating performance after MW sterilization process is heating uniformity, which, in this study, was defined as the difference between the hot spot and cold spots, i.e., $\Delta T_2 = (T_{\max} - T_{\min})_2$. The subscript 2 means the heating uniformity is calculated with respect to a two-dimensional plane since the focus was on the heat distribution in the middle layer of food packages. Obviously, a smaller ΔT_2 indicates better heating uniformity.

Four different cases summarized in Table 3 were used to illustrate the effectiveness of the validated simulation model in assisting the design of operation parameters to improve heating uniformity. P_1 and P_2 are input powers for the first and second MW sections, respectively. L is the distance between neighboring packages. In those cases, the input powers for the two cavities and the distance between the two neighboring food trays were deliberately changed to explore their effects on heating uniformity.

Fig. 8 shows the top view of two MW sections for the simulated moving food packages. The preheating and holding sections are presented in Fig. 1. Temperature profiles and distributions for each case were obtained using the FDTD model developed in this paper. These results are presented in Fig. 9a–d. The heating uniformity for each case was calculated based on the temperature difference between the hot and cold spots in the middle layer (xy-plane), as shown in Fig. 10.

The distance between the neighboring packages was kept the same in both Case 1 and 2, while the input power was changed for both MW cavities. In particular, the input power of the first microwave cavity was increased by 2.3 kW, and the input power of the second MW cavity was reduced by 0.7 kW. The heating uniformity was found to worsen by 30% from Case 1 to Case 2. The distance between the neighboring packages in Cases 3 and 4 was doubled from that used in Cases 1 and 2, and the effect of two different sets of input powers was investigated. From Fig. 10, the heating uniformities obtained in Case 3 and Case 4 were significantly improved as compared to those from Case 1 and Case 2. For example, when doubling the distance between two adjacent packages from Case 2 to Case 3, the temperature difference was changed from 13.6 °C to 7.7 °C, leading to heating uniformity improved by 43.4%. In addition, it was concluded that the closer the neighboring packages, the more sensitive the heating uniformity to the input power specified on cavities.

7. Conclusions

A model was developed to simulate MW sterilization processes for moving food packages in a 915 MHz pilot scale system by coupling EM and thermal phenomena. This model relied on the conformal FDTD technique to

solve the EM equations and a user-defined FDTD model for thermal field. By explicitly solving the coupled partial differential equations, the FDTD models intrinsically maintained the field continuity along the boundary between different media, and used a leap frog strategy to simulate MW heating in a representative moving package, which significantly reduced the computational complexity and simulation time. Direct temperature measurements and the patterns of color changes based on chemical marker M-2 formation in the whey protein gel were used to validate the simulation model. The validated model was used for four different cases to demonstrate its applications to improve heating uniformity by properly setting appropriate operational parameters such as input powers or gaps between moving packages.

Though only homogeneous food packages were considered in validating the model, the model can be easily extended for inhomogeneous food packages due to the explicit nature of FDTD method. In addition, the simulation results for homogeneous packages provided useful reference for studying the heating patterns for inhomogeneous food because of the single-mode system. For instance, the calculated temperature distributions showed which area had significant microwave energy focused and which area did not. Based on this information, inside an inhomogeneous food package, the dielectric properties could be deliberately altered so as to redirect surplus microwave to the area with less initial energy, which resulted in more uniform heating.

Acknowledgements

The authors acknowledge support from the USDA National Integrated Food Safety Initiative grant no. 2003-51110-02093 titled: Safety of foods processed using four alternative processing technologies and partial support from Washington State University Agriculture Research Center.

References

Balanis, C.A., 1989. Advanced Engineering Electromagnetics. John Wiley, New York.

Barratt, L., Simons, D., 1992. Experimental validation of a computer simulation of microwave heating. In: Proceedings of the 27th Microwave Power Symposium, pp. 118–122.

Bows, J., Patrick, M.L., Dibben, D.C., Metaxas, A.C., 1997. Computer simulation and experimental validation of phase controlled microwave heating. Presented at the 6th Microwave and High Frequency Heating Conference, Fermo, Italy.

Burfoot, D., Railton, C.J., Foster, A.M., Reavell, R., 1996. Modelling the pasteurization of prepared meal with microwave at 896 MHz. Journal of Food Engineering 30, 117–133.

Campbell, G.S., Calissendorff, C., et al., 1991. Probe for measuring soil specific-heat using a heat-pulse method. Soil Science Society of American Journal 55 (1), 291–293.

Chen, H., Tang, J., Liu, F., 2007. Coupled simulation of an electromagnetic heating process using the finite difference time domain method. Journal of Microwave Power and Electromagnetic Energy 41 (3), 50–68.

Clemens, J., Saltiel, G., 1995. Numerical modeling of materials processing in microwave furnaces. International Journal of Heat and Mass Transfer 39 (8), 1665–1675.

Dibben, D.C., Metaxas, A.C., 1994. Finite-element time-domain analysis of multimode applicators using edge elements. Journal of Microwave Power and Electromagnetic Energy 29 (4), 242–251.

Guan, D., Cheng, M., Wang, Y., Tang, J., 2004. Dielectric properties of mashed potatoes relevant to microwave and radio-frequency pasteurization and sterilization processes. Journal of Food Science 69 (1), E30–E37.

Gwarek, W.K., Celuch-Marcysiak, M., Sypniewski, M., Wieckowski, A., 1999. QuickWave-3D Software Manual. QWED, Poland.

Harms, P.H., Chen, Y., Mittra, R., Shimony, Y., 1996. Numerical modeling of microwave heating systems. Journal of Microwave Power and Electromagnetic Energy 31 (2), 114–121.

Harms, P.H., Lee, J.F., Mittra, R., 1992. A study of the nonorthogonal FDTD method versus the conventional FDTD technique for computing resonant frequencies of cylindrical cavities. IEEE Transactions on Microwave Theory and Techniques 40 (4), 741–746.

Holland, R., 1993. Pitfalls of staircase meshing. IEEE Transactions on Electromagnetic Compatibility 35 (4), 434–439.

Incropera, F.P., DeWitt, D.P., 2001. Introduction to Heat Transfer, fourth ed. John Wiley, New York.

Jurgens, T.G., Taflove, A., Umashankar, K., Moore, T.G., 1992. Finite-difference time-domain modeling of curved surfaces. IEEE Transactions on Antennas and Propagation 40 (4), 357–366.

Kopyt, P., Celuch-Marcysiak, M., 2003. Coupled electromagnetic and thermal simulation of microwave heating process. In: Proceedings of the 2nd International Workshop on Information Technologies and Computing Techniques for the Agro-Food Sector. Barcelona, November–December 2003, pp. 51–54.

Lau, M.H., Tang, J., Taub, I.A., Yang, T.C.S., Edwards, C.G., Mao, R., 2003. Kinetics of chemical marker formation in whey protein gels for studying microwave sterilization. Journal of Food Engineering 60 (4), 397–405.

Leo, R.D., Cerri, G., Mariani, V., 1991. TLM techniques in microwave ovens analysis: numerical and experimental results. In: Proceedings of the 1st International Conference on Computation in Electromagnetics, London, pp. 361–364.

Ma, L.H., Paul, D.L., Pothecary, N., Railton, C., Bows, J., Barratt, L., Mullin, J., Simons, D., 1995. Experimental validation of a combined electromagnetic and thermal FDTD model of a microwave-heating process. IEEE Transactions on Microwave Theory and Techniques 43 (11), 2565–2572.

Madsen, N.K., Ziolkowski, R.W., 1988. Numeric solution of Maxwell's equations in the time domain using irregular nonorthogonal grids. Wave Motion 10, 583–596.

Ohlsson, T., 1987. Sterilization of foods by microwaves. International Seminar on New Trends in Aseptic Processing and Packaging of Food stuffs, 22 October 1987; Munich. SLK Report No. 564. The Swedish Institute for Food and Biotechnology, Goteborg, Sweden.

Ohlsson, T., 1990. Controlling heating uniformity – the key to successful microwave products. European Food and Drink Review 2, 7–11.

Ohlsson, T., 1992. Development and evaluation of microwave sterilization process for plastic pouches. Paper presented at the AICHE Conference on Food Engineering, March 11–12, Chicago.

Osepchuck, J.M., 1984. A history of microwave heating applications. IEEE Transactions on Microwave Theory and Techniques MTT-32, 1200–1224.

Pandit, R.B., Tang, J., Liu, F., Mikhaylenko, M., 2007a. A computer vision method to locate cold spots in foods in microwave sterilization processes. Pattern Recognition 40 (2), 3667–3676.

Pandit, R.B., Tang, J., Liu, F., Pitts, M., 2007b. Development of a novel approach to determine heating pattern using computer vision and chemical marker (M-2) yield. Journal of Food Engineering 78 (2), 522–528.

Pandit, R.B., Tang, J., Mikhaylenko, G., Liu, F., 2006. Kinetics of chemical marker M-2 formation in mashed potato – A tool to locate

cold spots under microwave sterilization. Journal of Food Engineering 76 (3), 353–361.

Paoloni, F., 1989. Calculation of power deposition in a highly overmoded rectangular cavity with dielectric loss. Journal of Microwave Power and Electromagnetic Energy 24 (1), 21–32.

Pathak, S., Liu, F., Tang, J., 2003. Finite difference time domain (FDTD) characterization of a single mode applicator. Journal of Microwave Power and Electromagnetic Energy 38 (1), 37–48.

Ryynanen, S., Ohlsson, T., 1996. Microwave heating uniformity of ready meals as affected by placement, composition, and geometry. Journal of Food Science 61 (3), 620–624.

Shou-Zheng, Z., Han-Kui, C., 1988. Power distribution analysis in rectangular microwave heating applicator with stratified load. Journal of Microwave Power and Electromagnetic Energy 23 (3), 139–143.

Smyth, N.F., 1990. Microwave-heating of bodies with temperature-dependent properties. Wave Motion 12 (2), 171–186.

Speigel, R.J., 1984. A review of numerical models for predicting the energy deposition and resultant thermal response of humans exposed to electromagnetic fields. IEEE Transactions on Microwave Theory and Techniques MTT-32, 730–746.

Taflove, A., 1998. Computational Electrodynamics: The Finite-Difference Time-Domain Method. Artech House, Boston.

Tang, J., Liu, F., Pathak, S., Eves, G., 2006. Apparatus and method for heating objectives with microwaves. US Patent 7,119,313.

Torres, F., Jecko, B., 1997. Complete FDTD analysis of microwave heating processes in frequency-dependent and temperature-dependent media. IEEE Transactions on Microwave Theory and Techniques 45 (1), 108–117.

Watanabe, W., Ohkawa, S., 1978. Analysis of power density distribution in microwave ovens. Journal of Microwave Power and Electromagnetic Energy 13 (2), 173–182.

Webb, J.P., Maile, G.L., Ferrari, R.L., 1983. Finite element solution of three dimensional electromagnetic problems. IEE Proceedings 130 (2), 153–159.

Zhang, H., Datta, A.K., 2000. Coupled electromagnetic and thermal modeling of microwave oven heating of foods. Journal of Microwave Power and Electromagnetic Energy 35 (2), 71–85.